

Fundamentals of thermal convection II

When $Ra \gg Ra_{crit}$ thin thermal boundary layers surrounding the isothermal interior of a convection cell are formed. Based on this a scaling analysis can be performed to relate flow velocity and heat flow to Ra .

Boundary layer thickness δ versus velocity u

Model problem: consider column of fluid moving at the surface with characteristic velocity U in $+x$ -direction. $t=0$ is the time when it starts at the upwelling side, where it has a temperature $T(z')=T_i = \Delta T/2$ at all depths $z'=1-z > 0$. $T(z'=0)=0$, and by thermal conduction in the vertical direction, the column cools down to progressively larger depth (horizontal conduction is neglected).

$$\partial T / \partial t = \kappa \partial^2 T / \partial z'^2 ; \quad T(t=0, z') = T_i, \quad T(t, z'=0) = 0, \quad T(t, z' \rightarrow \infty) = T_i$$

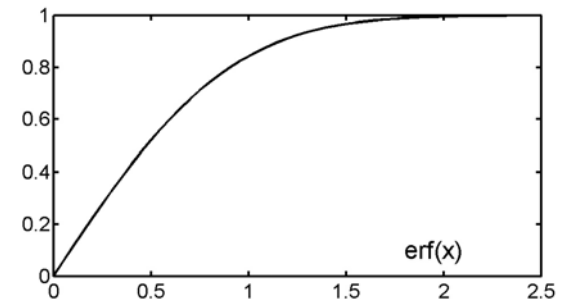
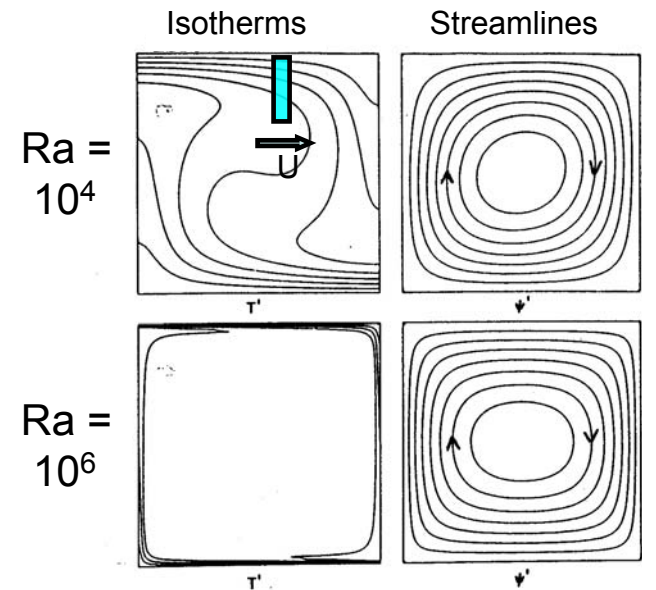
Introduce „similarity variable“ $\eta = z' / [2\sqrt{(\kappa t)}]$ to transform PDE into ODE

$$-\frac{1}{2} \eta \frac{dT}{d\eta} = \frac{d^2 T}{d\eta^2} ; \quad T(\eta=0) = 0, \quad T(\eta \rightarrow \infty) = T_i .$$

Solution: $T(\eta) = T_i \operatorname{erf}(\eta)$ where $\operatorname{erf}(x)$ is the error function.

At $\eta=1$, $\operatorname{erf}(\eta)$ has reached 84% of its asymptotic value; this can be taken to define the characteristic thickness of the boundary layer:

$$\delta = 2(\kappa t)^{1/2} = 2(\kappa x / U)^{1/2}$$



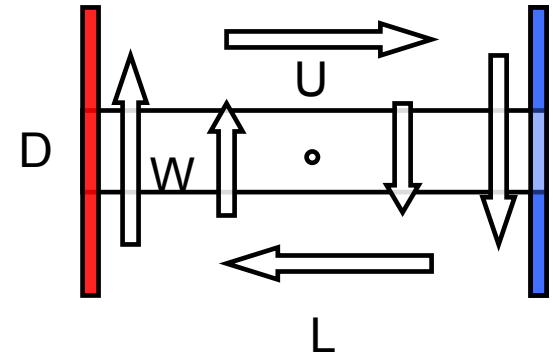
Symbols: δ – characteristic boundary layer thickness, U – characteristic velocity, z' – depth, T_i – temperature in core of convection cell, η – similarity variable

Boundary layer scaling

At the cell edge, the surface boundary layer with thickness $\delta = 2(\kappa L/U)^{1/2}$ bends around to form the cold vertical boundary layer of the descending flow (similarly the bottom/rising boundary layers). The buoyancy in the vertical boundary layers drives the flow.

Assume $w(x) \sim 2W (L/2-x)/L$. The associated shear stress is $\sigma_{xz} = \eta \partial w / \partial x \sim 2\eta W/L$. At the cell edge, this stress must be supplied by the action of the gravity force F_g due to the excess mass (or mass deficit) in the vertical boundary layers: $F_g/(A\delta) \sim \rho g \alpha \Delta T$. With $\sigma_{xz} = F_g/A \sim \rho g \alpha \delta \Delta T$ and $W \approx U$, $L \approx D$, we can combine all the results:

$$\eta U/D \sim \rho g \alpha \Delta T (\kappa D/U)^{1/2} \Rightarrow [UD/\kappa]^{3/2} \sim \alpha g \Delta T D^3 / (\kappa \nu)$$



In non-dimensional terms: $U \sim Ra^{2/3}$ $\delta \sim Ra^{-1/3}$ $Nu \sim Ra^{1/3}$

(Nusselt number: total / conductive heat flow, $Nu = Q / [k\Delta T/D]$, $Q \sim k\Delta T/\delta \Rightarrow Nu \sim D/\delta$)

A more quantitative analysis provides factors of proportionality, in case of $L = \sqrt{2} D$:

$$U = 0.33 Ra^{2/3} \quad \delta = 3.5 Ra^{-1/3} \quad Nu = 0.29 Ra^{1/3}$$

Symbols: W – characteristic vertical velocity, L – length of convection cell, F_g – gravity force of vertical boundary layer, σ_{xz} – shear stress, A – (unit) area of vertical boundary layer (facing in x-direction), Nu – Nusselt number, Q heat flow

Application to mantle convection

Results from boundary layer theory are applicable at sufficiently large value of Ra/Ra_c . Numerical simulations basically confirm the scaling results even though at high Rayleigh number the system shows chaotic time dependence and the exponents tend to be slightly smaller.

Range estimated for mantle convection $Ra \approx 4 \times 10^6 - 4 \times 10^7$

$U \approx 8 - 42$ cm/yr (observed plate velocities 5 -10 cm/yr)

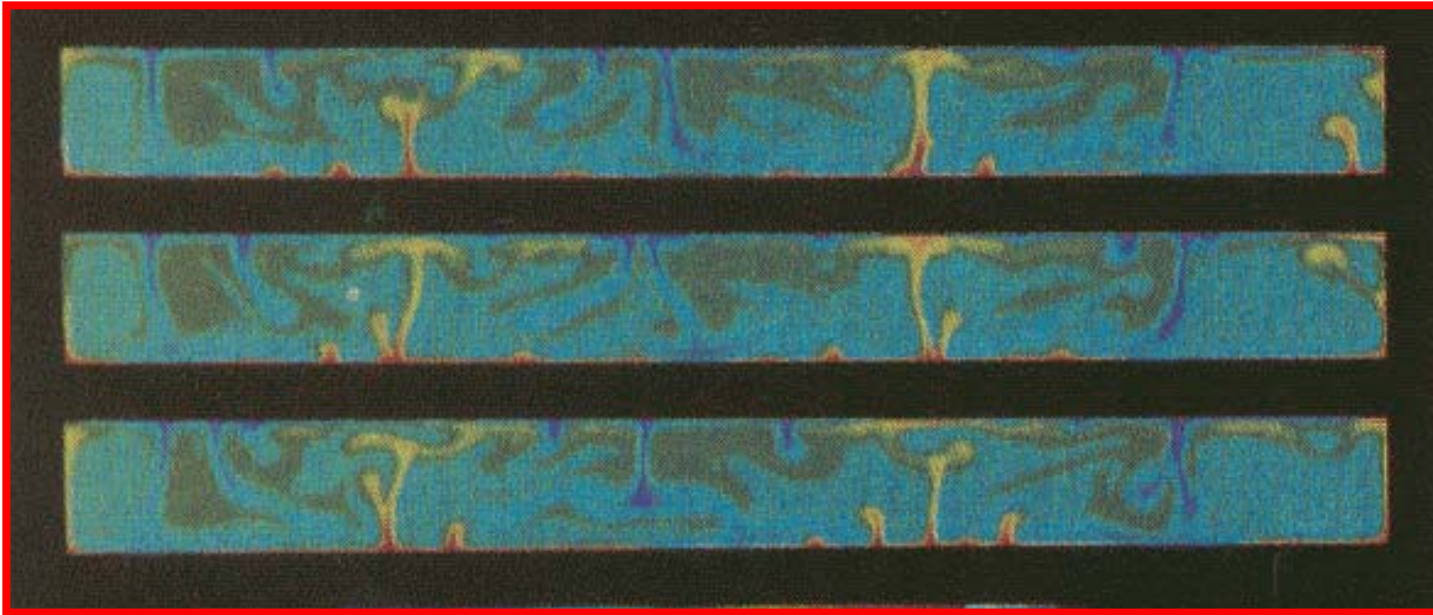
$Nu \approx 45 - 100 \Rightarrow Q \approx 120 - 260$ mW/m² (observed [oceans] 90 – 100 mW/m²)

$\delta \approx 31 - 66$ km (observed thickness of oceanic lithosphere 70 – 100 km)

Predictions are in the correct order of magnitude. They tend to be on the high side.

Differences may be caused by complications of mantle convection: Larger aspect ratio, viscosity variations, phase transitions, presence of continents, ...

High Rayleigh number convection



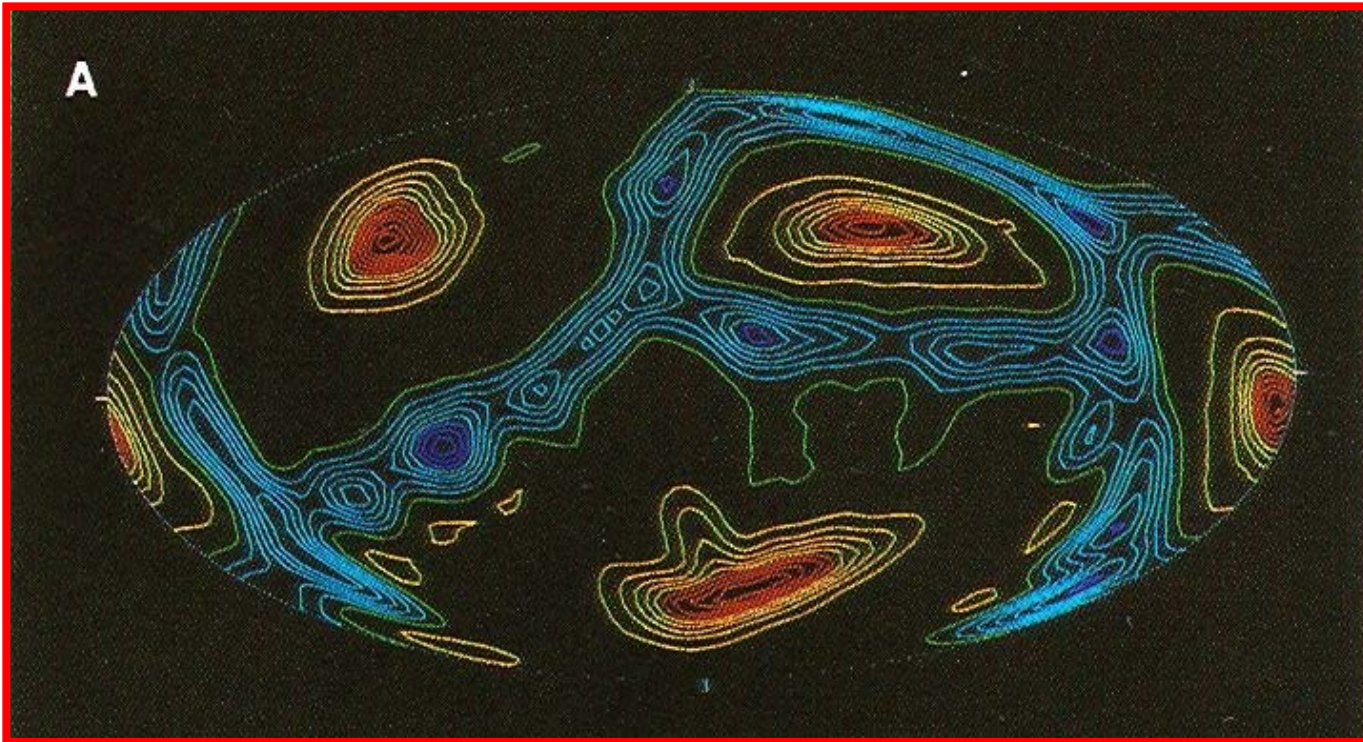
Numerical simulations in 2D and 3D basically confirm scaling laws, with slightly smaller values for exponents. At high Rayleigh number the flow shows chaotic time-dependence, with growing boundary layer instabilities: Local Rayleigh number condition for instability:

$$Ra_{\text{local}} = \alpha g \Delta T \delta^3 / (\kappa \nu) = Ra (\delta/D)^3 > Ra_{\text{crit}}$$

When in $\delta \sim Ra^{-\beta}$ the exponent $\beta < 1/3$, the boundary layer must eventually become unstable.

Smaller plumes growing in the boundary layers are swept into the main up/downwellings.

Planform of convection in a sphere



Radial velocity (red = rising, blue = sinking) near the outer boundary in a spherical convection model (Bercovici et al., JGR, 1989)

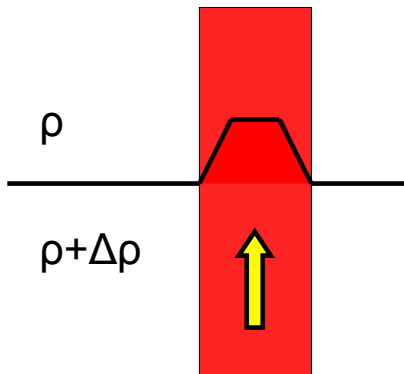
Numerical simulations of isoviscous convection in a spherical shell indicate that the hot rising flow takes the form of isolated plumes, whereas the cold sinking flow occurs in an interconnected network of sheets (not unlike subducting slabs).

Influence of phase transitions

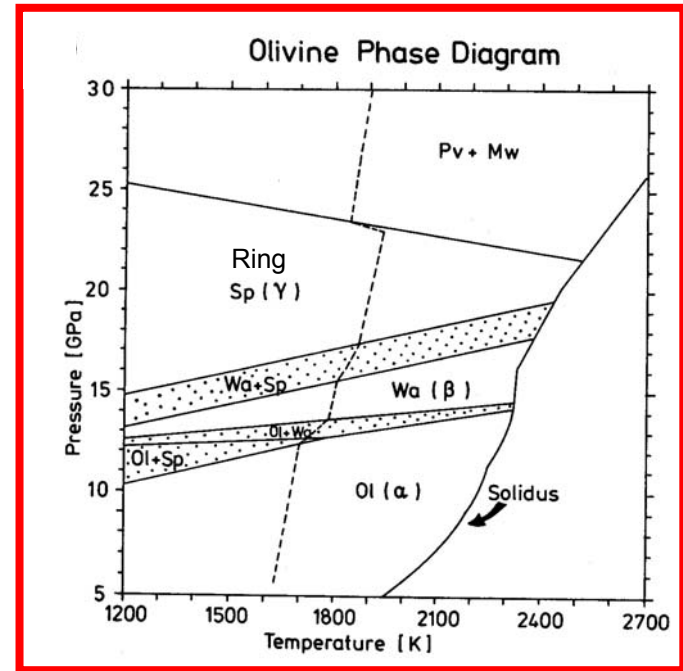
Solid-solid phase transitions at 410, 520 and 660 km depth, Olivine (α) \Rightarrow Wadsleyite (β) \Rightarrow Ringwoodite (γ) \Rightarrow Perovskite + Magnesiowüstite. Density change $\Delta\rho \approx 4 - 9\%$, Clapeyron slope $\gamma = dp/dT \approx +3 \text{ MPa/K}$ (410 km), -2.8 MPa/K (660 km).

Phase transitions influence convection by:

- (1) Release of latent heat ($Q_L = \gamma T \Delta\rho / \rho^2$), neglected in the Boussinesq approx.
- (2) Deflection of phase boundary in vertical boundary layers: $\delta z = -\gamma \delta T / (\rho g)$



Example: Deflection of phase boundary with $\gamma < 0$ in hot rising flow. Elevated region of high-density phase has negative buoyancy that opposes convection



Phase boundary with $\gamma > 0$ helps to drive convection, for $\gamma < 0$ it retards convection

Symbols: $\gamma = dp/dT$ – Clapeyron slope, Q_L – specific latent heat, $\Delta\rho$ – density contrast between phases, δT – temperature in boundary layer, δz – phase boundary deflection

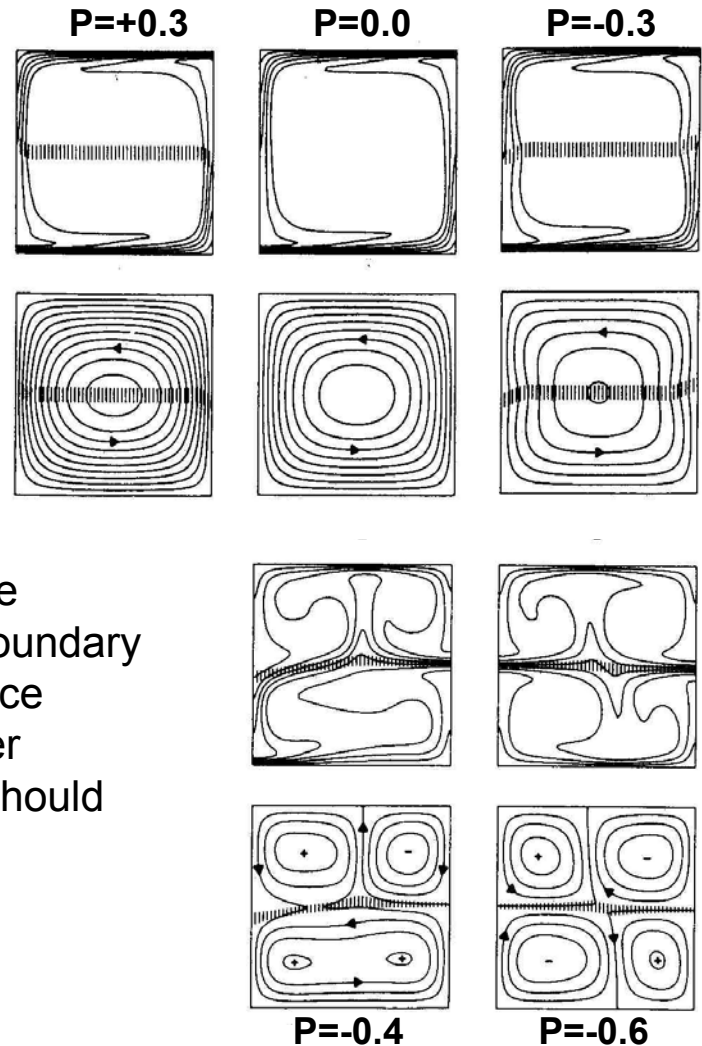
Influence of phase transitions II

Characteristic non-dimensional parameter obtained from balancing buoyancy force from phase boundary deflection, $-\Delta\rho g\delta z = \gamma\Delta\rho\delta T/\rho$, and that from thermal expansion, $\rho g\alpha\delta T D$:

$$P = \frac{\gamma \Delta\rho}{\rho^2 \alpha g D}$$

For $P < -1$, the opposing buoyancy of phase boundary deflection dominates over driving thermal buoyancy. The driving buoyancy is distributed over the entire vertical boundary layer, whereas the opposing buoyancy is localized. Hence single-layer convection breaks down in favor of two-layer convection at values $-1 < P < 0$. The critical value of P should depend on Ra (because b.-l.-thickness varies with Ra). Numerical results suggest

$$P_{\text{crit}} \approx -4.4 Ra^{-1/5}$$

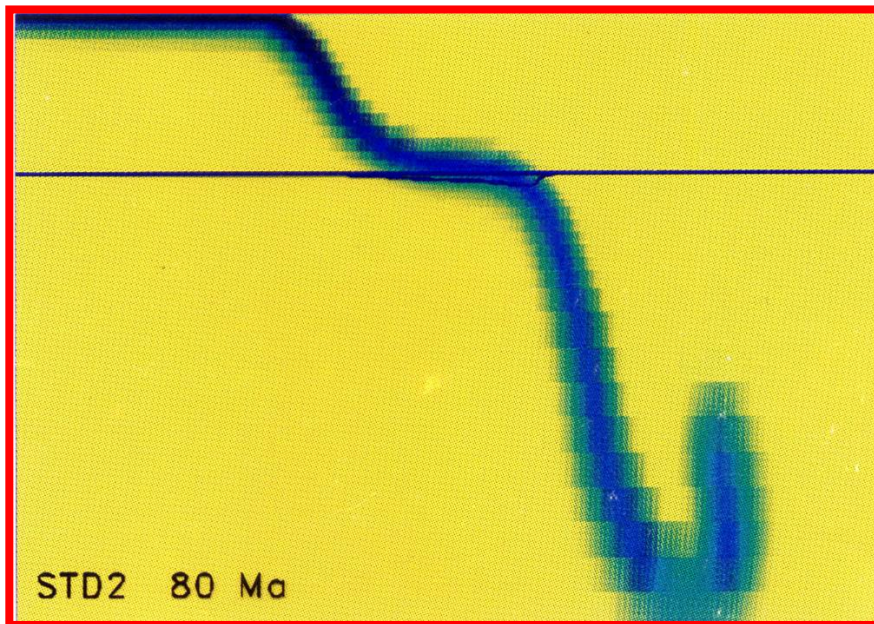


Symbols: $\gamma = dp/dT$ – Clapeyron slope, QL – specific latent heat, $\Delta\rho$ – density contrast between phases, δT – temperature in boundary layer, δz – phase boundary deflection

Phase transitions: Application to Earth

For the ringwoodite \Rightarrow perovskite+magnesiowüstite transition in the Earth $P \approx -0.1$.

For $Ra = 4 \times 10^6 - 4 \times 10^7$, $P_{crit} = -0.13$ to -0.21 . Hence the phase boundary is (marginally) unable to enforce layered convection, but has a sufficiently strong effect to generate complexity (such as retarded penetration of phase boundary).



Numerical simulation of a cold sinking lithospheric slab, interacting with a phase boundary with negative Clapeyron slope. Plate motion at 5 cm/yr and subduction is enforced by surface velocity conditions. There is retrograde motion of the point of descent (trench rollback) at -2 cm/yr. The slab is temporarily stopped at the phase boundary at 660 km depth because of its downward deflection at lower than normal temperature.

Symbols: $\gamma = dp/dT$ – Clapeyron slope, Q_L – specific latent heat, $\Delta\rho$ – density contrast between phases, δT – temperature in boundary layer, δz – phase boundary deflection

Phase transition: application to Mars

In Mars $g \approx 3.7 \text{ ms}^{-2} \Rightarrow$ pressure increases less rapidly with depth. Not clear if ringwoodite \Rightarrow perovskite+magnesiowüstite transition occurs above CMB. If it does, it is only some tens to 200 km above the CMB, i.e. in or close above the hot thermal boundary layer. $P \approx -0.4$ (larger than in Earth because of low g).



3D numerical simulation of convection in a sphere with phase boundary with negative P at short distance above the core. Starting from an initial condition with many rising plumes, the system evolves towards a convection pattern with one single plume (\Rightarrow Tharsis volcanism). The plumes are not stationary, but they migrate and they merge. Without the phase boundary, new plumes are formed by boundary layer instabilities. With the phase boundary, boundary layer instabilities are prevented from growth by the negative feedback of the phase boundary deflection.

